

Neutron Inelastic Scattering from Some Collective Nuclear States*

D. J. DONAHUE

Department of Physics, Pennsylvania State University, University Park, Pennsylvania

(Received June 18, 1962)

Fast neutrons from a reactor were used to produce, by inelastic scattering, excited states in various isotopes of Mg, Al, Ti, Cr, Fe, Cu, Zn, Mo, and Pb. The median energy of neutrons producing these excited states was approximately 2 to 3 MeV. Gamma rays emitted by the excited nuclei were observed with a NaI(Tl) crystal. After several corrections, the relative probabilities for exciting the various states by neutron inelastic scattering were obtained from the gamma-ray yields. A correlation is noted between the measured relative probability for exciting a nuclear state by neutron inelastic scattering and the reduced quadrupole transition probability, $B(E2)$, of that state, obtained from Coulomb excitation experiments.

I. INTRODUCTION

THE experiments described in this paper were performed to see if a correlation could be observed between the probability for exciting a nuclear state by neutron inelastic scattering and the collective properties of that state. Cohen, Price, and Rubin, using 23-MeV protons¹ and 15-MeV deuterons,² have observed a positive correlation between the cross section for exciting a nuclear state by inelastic scattering and the reduced quadrupole transition probability, $B(E2)$, of that state. The quadrupole transition probability of a state is considered to be a good measure of the degree to which that state has collective properties.² Pinkston and Satchler³ have shown that if one describes inelastic scattering with a direct interaction model, it is reasonable to expect that the cross section for exciting a nuclear state which can decay by emission of gamma radiation of multipolarity EL is proportional to $B(EL)$. That is, they show that σ_L (inelastic scattering) $\propto B(EL)$.

In this work, fast neutrons in a beam from a nuclear reactor were used to excite discrete nuclear states in a number of isotopes, ranging from Mg²⁴ to Pb²⁰⁶. Neutrons of all energies up to about 12 MeV are present in this beam. However, the number of neutrons per unit energy decreases exponentially with increasing neutron energy. Also, the neutron inelastic scattering cross sections, in general, rise rapidly as neutron energy increases, from zero at threshold to nearly a constant. Therefore, the median energy of the neutrons causing a given reaction is from 1 to 2 MeV above the threshold energy of that reaction. For most of the nuclear states investigated here, the threshold energy was about 1 MeV, and the median energy of the neutrons causing the reactions was about 2 to 3 MeV. The particular isotopes used were selected because they each have an excited state with an energy greater than 0.7 MeV, which can decay to the ground state by emission of electric quadrupole radiation, and for which transition the value of $B(E2)$ has been measured, usually by Coulomb excitation experiments. The yield of γ rays

emitted at a given angle with respect to the incident neutrons was measured for each of these states, and, after being subjected to appropriate corrections, was compared to the previously determined values of $B(E2)$ of the state. A definite correlation between the two quantities is noted.

II. EXPERIMENTAL PROCEDURE

A. General

The experimental arrangement was similar to one described previously.⁴ Fast neutrons from a pool reactor passed through a beam hole in a concrete wall, and were incident on a target located about 12 ft from the reactor. The beam hole contained an iron collimator, 30 in. long, which restricted the diameter of the neutron beam at the target to about 2 in. A 4-in.-thick bismuth plug and a 6-in.-thick lithium fluoride-paraffin plug were placed in the beam to reduce, respectively, the number of γ rays and thermal neutrons in the beam. Gamma rays produced in the target were detected with a 3-in.-diam, 3-in.-length NaI(Tl) crystal, and the pulses from the photomultiplier were recorded in a 128-channel pulse-height analyzer. The crystal was located 15 in. from the target, at a position such that the angle between the incident beam and the γ rays which were detected was about 120°.

Figure 1 shows the energy spectrum of γ rays obtained from an iron target. The nuclear γ rays seen are identified as: (a) 0.85-MeV γ rays emitted in transitions from the 2⁺ first-excited state of Fe⁵⁶ to the ground state, (b) 1.24-MeV γ rays from transitions from the first 4⁺ state to the first 2⁺ state in Fe⁵⁶, and (c) 1.82-MeV γ rays from transitions between the second and the first 2⁺ states in Fe⁵⁶. The intensity of any other nuclear γ rays in the spectrum is less than 5% of that of the 0.85-MeV γ rays. The γ rays at 0.51 MeV result from the annihilation of positrons produced in the target by γ rays in the beam. This spectrum from iron is, in some ways, typical of the spectra obtained from most of the even- A targets investigated. The most intense γ rays observed from these targets always resulted from 2⁺→0⁺ transitions. Additional γ rays, probably from 4⁺→2⁺

* Supported in part by the U. S. Atomic Energy Commission.

¹ B. L. Cohen and A. G. Rubin, Phys. Rev. **111**, 1568 (1958).

² B. L. Cohen and R. E. Price, Phys. Rev. **123**, 283 (1961).

³ W. T. Pinkston and G. R. Satchler, Nuclear Phys. **27**, 270 (1961).

⁴ D. J. Donahue, Phys. Rev. **124**, 224 (1961).

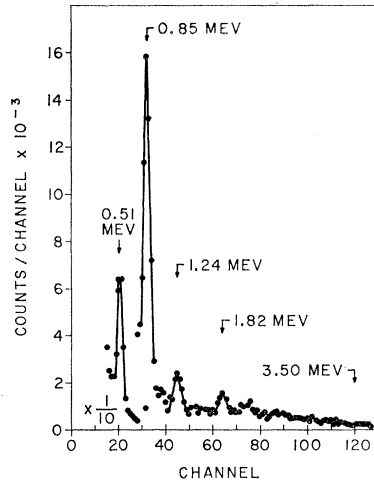


FIG. 1. Pulse-height spectrum from an iron target.

transitions and from $2^+ \rightarrow 2^+$ transitions were usually observed, and the sum of the intensities of these γ rays was about 0.3 of the intensity of the γ rays from the $2^+ \rightarrow 0^+$ transition. That no other γ rays from transitions from higher energy states were observed can be explained, in part, by the fact the number of high-energy neutrons in the beam from the reactor decreases approximately exponentially with increasing neutron energy.

From Fig. 1 we obtain the areas under the peaks of the three γ rays. After correcting these areas for differences in γ -ray absorption in the target and for differences in crystal efficiency, the areas of the 1.24- and 1.82-MeV peaks are subtracted from that of the 0.85-MeV peak. The result is a quantity which is proportional to the rate of production, per target nucleus, of the 0.85-MeV state in Fe^{56} . A similar quantity was measured for the first 2^+ states in Mg^{24} , Mg^{26} , Ti^{48} , Cr^{52} , Mo^{96-98} , Pb^{206} , and the even- A isotopes of zinc. Measurements were also made for some states which can decay by emission of electric quadrupole radiation in Mg^{26} , Al^{27} , Cu^{63} , and Cu^{65} .

Before the relative rates of production of these states can be compared with their known values of $B(E2)$, several corrections must be considered. Corrections for differences in absorption of the different γ rays in the target material, and for differences in crystal efficiency were made in a straightforward manner. No correction was made for multiple scattering of neutrons in the target. Each had a thickness of less than 0.2 mean free path for elastic scattering, and it was assumed that the increase in path length in the target from elastic scattering was just compensated by a decrease in flux due to inelastic scattering. Day⁵ has stated that this assumption is, in some cases, nearly correct.

Since only γ rays emitted at about 120° to the incident neutron beam were detected, a correction for differences in angular distributions was considered. Angular dis-

tributions of the γ rays from Mg^{24} , Ti^{48} , and Fe^{56} were measured and found to be nearly the same. Further, for all angular distributions which could be reasonably expected, the γ -ray yield per unit solid angle at 120° is very nearly (within a few percent) the same fraction of the total yield. Therefore, no correction has been made to the data presented here for differences in angular distributions.

One further correction must be made to account for the fact that, because the thresholds of the reactions producing the various nuclear states are different, while the neutron energy spectrum is continuous, each sample sees a different effective neutron flux. The flux at energies greater than about 1 MeV from a pool reactor can be described⁶ by the equation $\Phi(E) = \Phi_0 e^{-\alpha E}$, where Φ_0 and α are constants. The parameter α depends on the material in the beam hole, and for our arrangement it is almost certainly between 0.4 and 0.6 MeV^{-1} .⁶ Measurements of the energy dependence of neutron inelastic-scattering cross sections⁷ show that, in general, these cross sections rise rapidly above threshold and approach a constant value. We assume that for energies greater than E_{th} , the threshold energy, $\sigma(E)$ can be written.

$$\sigma(E) = \sigma_\infty (1 - e^{-\beta(E - E_{\text{th}})}), \quad (1)$$

where σ_∞ is a constant, but different for each reaction, and β is a parameter which is the same for all reactions. A value of β which is consistent with most available measurements is $\beta = 3 \pm 1 \text{ MeV}^{-1}$. That is, the cross sections for most states reach about two-thirds of their maximum values between 250 and 500 keV above threshold.

The corrected rate of production of a state Y is then written

$$Y = RF, \quad (2)$$

where R is the rate of production of the state, measured as described above, and F is the flux correction factor. If the flux seen by each state is corrected to that seen by a state with a threshold at 1 MeV, then

$$F = e^{\alpha(E_{\text{th}} - 1)}, \quad (3)$$

where E_{th} is in MeV, and α is taken to be $0.5 \pm 0.1 \text{ MeV}^{-1}$. If Eq. (1) is a reasonable description of neutron inelastic cross sections, then the corrected yield Y is proportional to the asymptotic value of the inelastic cross section, σ_∞ .

Several comments concerning this correction should be made. The assumption that the parameter β is the same for all the reactions investigated might seem rash, but if the values of β are between 2 and 4 MeV^{-1} , the correction factor F will be accurate to about 5%. An uncertainty of 0.1 MeV^{-1} in α results in an uncertainty in F of less than 2% for most of the cases treated here. Since the cross sections of the silicon isotopes exhibit

⁶ *Research Reactors* (McGraw-Hill Book Company, Inc., New York, 1955), pp. 108-111.

⁷ D. A. Lind and R. B. Day, *Ann. Phys. (New York)* **12**, 485 (1961).

⁵ R. B. Day, *Phys. Rev.* **102**, 767 (1956).

resonances,⁷ the validity of the correction factor might seem dubious when applied to the magnesium and aluminum data. However, the continuous nature of the neutron spectrum insures that we measure only average cross sections, and such averages, even for low- A isotopes could well be described by Eq. (1). Finally, it should be noted that only for the magnesium and chromium isotopes does the correction factor, F , differ from unity by more than 10%. Therefore, even though the assumptions made to obtain F may not be completely justified, they should not seriously affect the over-all conclusions of this experiment.

B. Specific Cases

Most of the difficulty encountered in obtaining the relative yields of particular excited states resulted from uncertainties in subtracting background from the signal, and in correcting for contributions to the signal of cascades from higher states. Data from each of the targets are discussed below.

Iron

Figure 2 shows the spectrum of γ rays obtained when a sample of about 100 g of iron was placed in the neutron beam. The energy scale in this figure is different from that of Fig. 1. Also shown in the figure is an energy level diagram of Fe^{56} , illustrating the states which were produced by neutron inelastic scattering. The solid line in the figure represents our estimate of the background which must be subtracted from the signal. The area under each of the three peaks was determined by using the sum of the counts in five channels around the peak energy, and by assuming that these five channels were part of a Gaussian distribution of known shape. From these areas, the relative rate of production of the 0.85-MeV, 2^+ state in Fe^{56} by neutron inelastic scattering was obtained in the manner described above. The spectrum from Fe^{56} is one of the best that was obtained in these experiments, and the estimated uncertainty in the area corresponding to the cross section for production of the 0.85-MeV state is less than 10% of that area.

Titanium

The spectrum from titanium was quite similar to that from iron. All of the γ rays observed could be identified with transitions in Ti^{48} . In addition to a 0.99-MeV γ ray, emitted in the transition from the first 2^+ state to the ground state, γ rays with energies of 1.31 and 1.45 MeV were observed, corresponding, respectively, to transitions from the first 4^+ and the second 2^+ states to the first 2^+ state in Ti^{48} . The intensities of these two transitions were, respectively, 14 and 11% of that of the $2^+ \rightarrow 0^+$ transition.

Magnesium

From a target of natural magnesium, γ rays with energies of 1.37, 1.8, and 1.6 MeV were observed. These

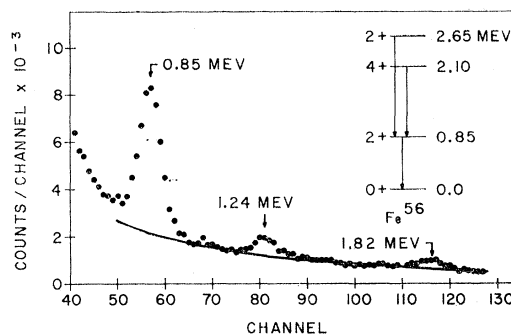


FIG. 2. Pulse-height spectrum from an iron target. The solid line represents the background to be subtracted from the signal.

correspond to transitions from the first 2^+ state to the ground state in Mg^{24} and Mg^{26} , and from the third-excited state to the ground state in Mg^{25} . No other γ rays were seen. However, the 1.6- and 1.8-MeV peaks were very small, and weak transitions in Mg^{25} or Mg^{26} could not have been seen. Because the signals from states in Mg^{25} and Mg^{26} were so weak, the uncertainty in the measured rate of production of these two states is about 25% of the rate.

Aluminum

Gamma rays with energies of 0.85, 1.01, and 1.7 MeV were observed from an aluminum target. They were assumed to result from transitions from the first- and second-excited states of Al^{27} to the ground state, and from the state in aluminum at 2.7 MeV to the second-excited state.

Copper

Yields were measured of γ rays emitted in transitions from the 0.96-MeV state to the ground state of Cu^{63} and from the 1.11-MeV state to the ground state in Cu^{65} . Other weak γ rays were produced in the natural copper target, but none were seen which could be identified as belonging to a cascade from a higher energy state to the states in question. A study of the level diagrams of Cu^{63} and Cu^{65} indicates that such cascades are improbable, and no cascade corrections were made.

Chromium

Figure 3 shows the γ -ray spectrum obtained from a chromium target, with the background subtracted from the points. The solid curve is the shape of the line expected from 1.43-MeV γ rays. Gamma rays with energies of 1.72, 1.43, and 0.95 MeV are clearly seen. There is also an indication of a weak γ ray at 1.33 MeV. Wilson *et al.*⁸ have recently published the results of a comprehensive investigation of the level structure of Cr^{52} . They report levels at 1.43, 2.37, and 2.76 MeV, with quantum numbers 2^+ , 4^+ , and 4^+ . We identify the 1.43-, 0.95-, and 1.33-MeV γ rays in the spectrum in

⁸ R. R. Wilson, A. A. Bartlett, J. J. Kraushaar, J. D. McCullen, and R. A. Ristinen, *Phys. Rev.* **125**, 1655 (1962).

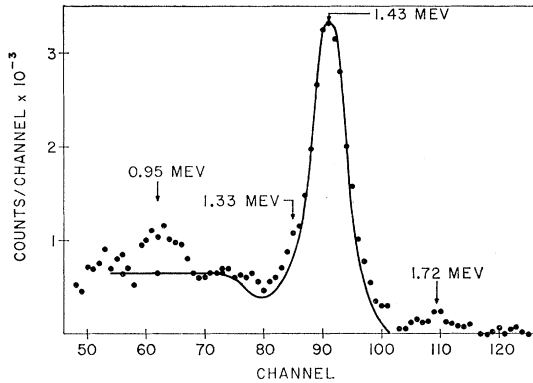


FIG. 3. Pulse-height spectrum from a chromium target, with background subtracted. The solid curve shows the expected shape of a spectrum produced by 1.43-MeV gamma rays.

Fig. 3 with $2^+ \rightarrow 0^+$, $4^+(2.37) \rightarrow 2^+$, and $4^+(2.76) \rightarrow 2^+$ transitions. The 1.72-MeV γ rays are assumed to result from transitions from the 3.16-MeV level in Cr^{52} , reported by Wilson *et al.*, to the 1.43-MeV level. If the inelastic scattering process in Cr^{52} is similar to that in Fe^{56} and Ti^{48} , the 3.16-MeV level could be the second 2^+ level in Cr^{52} .

Figure 3 illustrates the difficulty encountered in correcting for cascades. The sum of the intensities of the 0.95-, 1.33-, and 1.72-MeV γ rays is only about one-fourth of the intensity of the 1.43-MeV γ -rays. However this sum is uncertain by nearly a factor of 2, and thus the cascade correction introduces an error of about 10% in the rate of production of the 1.43-MeV state.

Zinc

The spectrum from a target of natural zinc is illustrated in Fig. 4. Zinc has three even- A isotopes, Zn^{64} , Zn^{66} , and Zn^{68} which make up 95.3% of the natural abundance. Each of these isotopes has a 2^+ level at about 1.0 MeV. The $B(E2)$ values for these levels are nearly equal⁹ so that, in this work, they can be treated as a single level. However, as shown in Fig. 4, the width

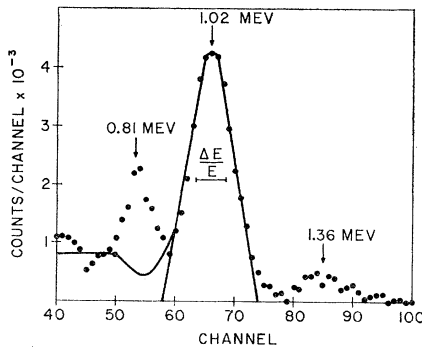


FIG. 4. Pulse-height spectrum from a zinc target. Background has been subtracted.

⁹ I. Kh. Lemberg, in *Reactions Between Complex Nuclei*, edited by A. Zucker, F. T. Howard, and E. C. Halbert (John Wiley & Sons, Inc., New York, 1960), p. 112.

of the line resulting from the three γ rays is greater than that expected from the resolution of the crystal. Therefore, instead of using an area computed from a few points and the known shape of the line, the area enclosed by the triangular curve in Fig. 4 was used. To compare the yield of 1.0-MeV γ rays from Zn to that of γ rays from other targets, similar areas must, of course, be used for the other γ rays.

In addition to the 1.0-MeV γ rays from the $2^+ \rightarrow 0^+$ transitions in zinc, γ rays with energies of about 0.81 and 1.36 MeV were observed, with intensities of about 20 and 12%, respectively, of the 1.0-MeV yield. The shape of the curve from the 1.0-MeV γ rays which was used in computing these intensities is shown in Fig. 4. We assume that these γ rays were emitted in transitions to the 2^+ states from known levels in the even- A isotopes of zinc at about 1.85 and 2.3 MeV.

Molybdenum

The interpretation of data from molybdenum is complicated by the fact that this element has seven

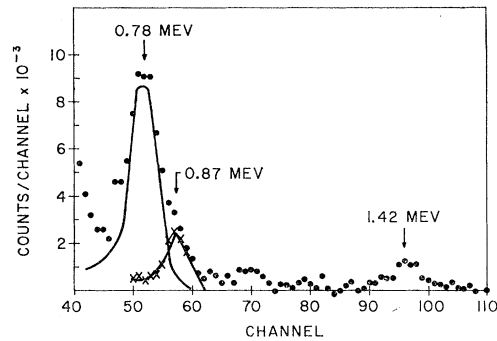


FIG. 5. Pulse-height spectrum from a molybdenum target. Background has been subtracted.

isotopes, all of which occur with appreciable abundances. The isotopes Mo^{96} and Mo^{98} , which are about 40% of natural molybdenum, have 2^+ levels at 0.78 MeV. The $B(E2)$ values for these two levels are nearly equal, and since they are larger than those of any other levels which could be studied in these experiments, we have tried to obtain some information from these levels.

Figure 5 shows the spectrum obtained from a molybdenum target, after the background from the target is removed. The shape of the solid curve centered at channel 52 is that which would be expected from γ rays with energies of 0.78 MeV. The x 's are the remainders after this solid curve is subtracted from the data. As can be seen, there are peaks at 0.78 and 0.87 MeV, as well as one at 1.42 MeV. The 0.78-MeV peak results mainly from $2^+ \rightarrow 0^+$ transitions in Mo^{96} and Mo^{98} . The 0.87-MeV peak results from a $2^+ \rightarrow 0^+$ transition in Mo^{94} and probably from transitions to the 2^+ states from states at about 1.65 MeV in Mo^{96} and Mo^{98} . Because γ rays from cascade transitions in Mo^{96} and Mo^{98} have nearly the

same energies as the γ rays emitted in the $2^+ \rightarrow 0^+$ transition in Mo^{94} , it was not possible to measure the contribution of cascades to the intensity of the 0.78-MeV γ rays. Rather, we have assumed that the contribution of cascades from higher levels to the intensity of the 0.78-MeV γ rays is equal to the average of the contribution of cascades to the $2^+ \rightarrow 0^+$ transition in Fe^{56} , Ti^{48} , Cr^{52} , and $\text{Zn}^{64-66-68}$. With an arbitrarily chosen uncertainty of 50%, this results in a correction for cascades to the yield of the 0.78-MeV γ rays of $28 \pm 14\%$.

Finally, the possibility that some of the 0.78-MeV γ rays come from isotopes other than Mo^{96} and Mo^{98} must be considered. A γ ray from Mo^{92} , with an energy of 0.79 MeV, has been assigned¹⁰ to a $4^+ \rightarrow 2^+$ transition in that element. We estimate that this γ ray could contribute, at most, 5% of the intensity of the observed 0.78-MeV peak. Mo^{95} has a group of states near 0.78 MeV.¹¹ However, these states decay predominantly through a state at 0.20 MeV. McGowan and Stelson¹² observed no 0.78-MeV γ rays from inelastic scattering of protons by Mo^{95} . No other likely sources of 0.78-MeV γ rays were found, and we therefore assume that all of the observed 0.78-MeV γ rays result from $2^+ \rightarrow 0^+$ transitions in Mo^{96} and Mo^{98} .

*Pb*²⁰⁶

Figure 6 shows the data obtained from a radiolead target (88% Pb^{206}). The background, indicated by the solid curve, was difficult to fix, because of its rapid increase at energies less than about 1 MeV. This rise probably results from bremsstrahlung produced by beta particles emitted by RaE (Bi^{210}) in the target. The only γ rays seen are a weak one at 1.36 MeV and one or more strong ones at about 0.8 MeV. Figure 7 shows the results of Fig. 6, near 0.8 MeV, after the background is removed. The dots are experimental points, the solid curve is the shape expected from 0.8-MeV γ rays, and the crosses are the remainder after the solid curve is subtracted from the experimental points. The dashed curve is the one which would be expected from 0.87-MeV γ rays with an intensity one-fourth that of the 0.80-MeV γ rays. The 0.80-MeV peak is assigned to the $2^+ \rightarrow 0^+$ transition in Pb^{206} , and the 0.87-MeV peak to the transition from the 4^+ state in Pb^{206} at 1.68 MeV¹³ to the 2^+ state. The 1.36-MeV γ rays are assumed to be emitted from the 2.16-MeV state⁷ in Pb^{206} .

It has been shown⁷ that a 3^+ state in Pb^{206} at 1.34 MeV is strongly excited by neutron inelastic scattering. Because of the 0.51-MeV peak in the background, we could not observe the 0.54-MeV γ rays emitted when this state decays to the 2^+ state. Rather, we have used Lind and

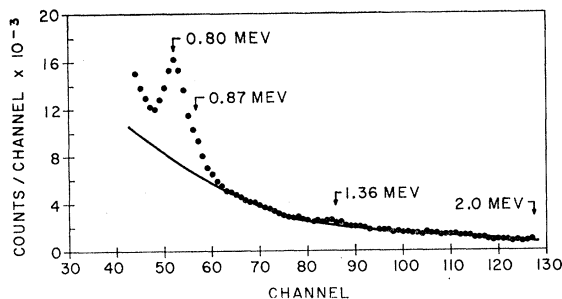


Fig. 6. Pulse-height spectrum from a target of radiolead. The solid curves shows the assumed background.

Day's results⁷ to correct our data. They found that at neutron energies above 1.6 MeV, the 0.54-MeV γ rays were produced with an intensity of about 30% of that of the 0.8-MeV γ rays. Application of the flux correction factor to account for the fact that the threshold of the 3^+ state is 0.54 MeV greater than that of the 2^+ state, gives the result that 23% of the 0.8-MeV γ rays from Pb^{206} come from cascades from the 3^+ level at 1.34 MeV. This result is assumed to be uncertain by 50%. The large and uncertain corrections for cascades from higher states to the first 2^+ state in Pb^{206} , and the uncertainty in subtracting the background, result in an uncertainty in the corrected yield of this state of nearly 33% of that yield.

III. RESULTS AND DISCUSSION

A summary of the results of these experiments is presented in Table I. Column 2 of the table gives the intensities, in arbitrary units, of the γ rays emitted in the transitions listed in column 1. Column 3 gives the

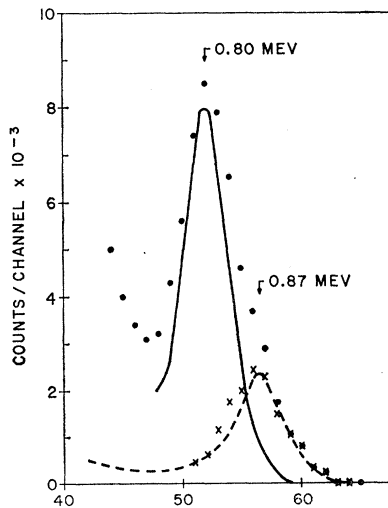


Fig. 7. Spectrum from radiolead with background subtracted. The points are the experimental data, the solid curve is the shape expected from 0.8-MeV gamma rays, and the x 's are the difference between the points and the solid curve. The dashed curve is that expected from 0.87-MeV gamma rays which have an intensity one-fourth of that of the 0.8-MeV gamma rays.

¹⁰ R. van Lieshout, S. Monaro, G. B. Vingiani, and H. Morinaga, *Bull. Am. Phys. Soc.* **7**, 342 (1962).

¹¹ J. P. Unik and J. D. Rasmussen, *Phys. Rev.* **115**, 1687 (1959).

¹² F. K. McGowan and P. H. Stelson, *Phys. Rev.* **109**, 901 (1958).

¹³ D. E. Alburger and M. H. L. Pyrcce, *Phys. Rev.* **95**, 1482 (1954).

TABLE I. Experimental results.

Transition	Intensity (arbitrary units)	Cascade intensity (arb. units)	Flux correction F	Corrected yield Y	$B(E2)$ ($e^2 \times 10^{-48} \text{ cm}^4$)
Mg ²⁴ (1.37 MeV)	29.3	...	1.20	35±5	0.05 ^{a,b}
Mg ²⁵ (1.6 MeV)	13.3	...	1.35	18.0±4.5	0.013 ^c
Mg ²⁶ (1.8 MeV)	27.6	...	1.49	41±10	0.03 ^c
Al ²⁷ (0.85 MeV)	6.85	...	0.93	6.4±1.4	0.0016 ^{a,b}
Al ²⁷ (1.01 MeV)	12.5	2.3	1.00	10.2±1.5	0.003 ^{a,b}
Ti ⁴⁸ (0.99 MeV)	67	17	1.00	50±7	0.07 ^{a,d}
Cr ⁵² (1.43 MeV)	53	12	1.24	51±8	0.06 ^{a,e}
Fe ⁵⁶ (0.85 MeV)	68	20	0.93	45±5	0.09 ^{a,b,e,f,g}
Zn ⁶⁴⁻⁶⁶⁻⁶⁸ (1.02 MeV)	84	25	1.00	59±10	0.11 ^{a,g}
Cu ⁶³ (0.96 MeV)	28.7	...	0.98	28±5	0.029 ^g
Cu ⁶⁵ (1.11 MeV)	29.4	...	1.05	31±6	0.027 ^g
Mo ⁹⁶⁻⁹⁸ (0.78 MeV)	120	34	0.90	77±16	0.28 ^h
Pb ²⁰⁶ (0.80 MeV)	123	70	0.91	48±15	0.135 ⁱ

^a Reference 9.
^b Reference 14.
^c Reference 15.

^d Reference 16.
^e Reference 17.
^f Reference 18.

^g Reference 19.
^h Reference 20.
ⁱ Reference 21.

intensities of the cascade γ rays which must be subtracted from column 2, and column 4 lists the flux correction factors, F , by which the differences of column 2 and 3 are multiplied. The corrected yields, Y , which are proportional to the relative probabilities per target nucleus for exciting the states listed in column 1, are given in column 5, and the $B(E2)$ values,^{9,14-21} in units $e^2 \times 10^{-48} \text{ cm}^4$, are listed in column 6. In general, when the results of more than one measurement of a given $B(E2)$ value are available, the average of the various measurements is used. However, for Ti⁴⁸ the average of two recent measurements was used, and the value of an earlier measurement was not.

The errors listed for the corrected yields are our estimates of the standard deviations of these yields. As indicated above, they result primarily from uncertainties in subtracting background radiation and in correcting for cascades from higher levels through the state in question. No error has been included for uncertainties in the flux correction factor, F . No errors have been listed for the $B(E2)$ values. Most of them are quoted with errors of between 10 and 20%.

The corrected yields of the various states are plotted vs the $B(E2)$ values of those states in Fig. 8. The straight line in the figure is a least square fit to the data,

obtained with the assumption that the errors for the $B(E2)$ values are zero. The slope of this line is 0.48, and its standard derivation is 0.02, so that the data are best described by the equation $Y = (\text{const})[B(E2)]^{0.48 \pm 0.02}$. Only the points for Mg²⁶ and Cr⁵² are more than one standard deviation away from the line, so the fit of the data to this line must be considered very good. More quantitatively, the value of "chi square"²² of the fit is only 0.6 of the expected value.

Schrank *et al.*²³ have suggested that a relationship between $\sigma(\text{inelastic})$ and $B(E2)$ should include the factor A , the mass number of the nucleus being studied. We have tried to fit the data in Table I to an expression of the form

$$Y = a[A^n B(E2)] + b, \quad (4)$$

where a , b , and n are free parameters. An equation of this form fits the data best when $n = -\frac{1}{2}$. Figure 9 illustrates the measured yields plotted against the

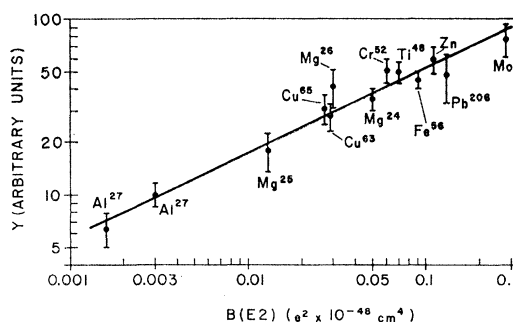


FIG. 8. The measured relative probability Y for exciting a nuclear state by neutron inelastic scattering vs the $B(E2)$ value of that state. The straight line is a least-square fit to the data.

¹⁴ H. E. Gove and C. Broude in *Reactions Between Complex Nuclei*, edited by A. Zucker, F. T. Howard, and E. C. Halbert (John Wiley & Sons, Inc., New York, 1960), p. 57.

¹⁵ V. K. Rasmussen, F. R. Metzger, and C. P. Swann, *Phys. Rev.* **123**, 1386 (1961).

¹⁶ V. Knapp, *Proc. Phys. Soc. (London)* **71**, 194 (1958).

¹⁷ B. M. Adams, D. Eccleshall, and M. J. L. Yates, in *Reactions Between Complex Nuclei*, edited by A. Zucker, F. T. Howard, and E. C. Halbert (John Wiley & Sons, Inc., New York, 1960), p. 95.

¹⁸ F. Metzger, *Nuclear Phys.* **27**, 612 (1961).

¹⁹ G. M. Temmer and N. P. Heydenberg, *Phys. Rev.* **104**, 967 (1956).

²⁰ R. H. Stelson and F. K. McGowan, *Phys. Rev.* **110**, 489 (1958).

²¹ P. H. Stelson and F. K. McGowan, *Phys. Rev.* **99**, 112 (1955).

²² P. Cziffra and M. J. Moravcsik, University of California Radiation Laboratory Report UCRL-8523 Rev. (unpublished).

²³ G. Schrank, E. K. Warburton, and W. W. Daehnick, *Phys. Rev.* **127**, 2159 (1962).

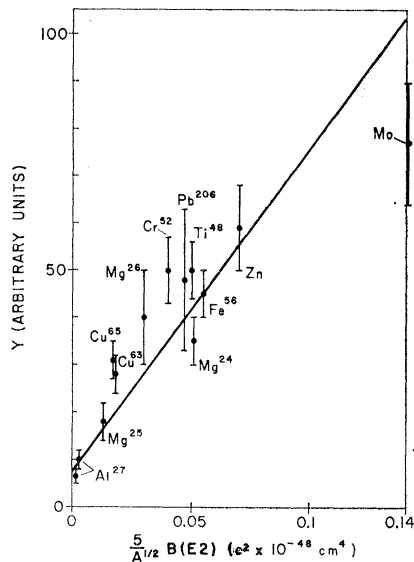


FIG. 9. The measured relative probability Y for exciting a nuclear state by neutron inelastic scattering vs the quantity $5A^{-1/2}B(E2)$ for that state. The straight line is a least-square fit of the type described in the text.

quantity $5A^{-1/2}B(E2)$, together with the line which gives the best fit to the data. As can be seen, the deviations of the data from this line are greater than those

in Fig. 8. The chi-square value of the fit is 2.2 times the expected value. The best fits to the data when the parameter n in Eq. (4) is 0.0 and -1.0 , have, respectively, chi-square values of 3.1 and 3.6 times the expected value. To summarize, if Eq. (4) is considered a valid expression for all of the data presented in Table I, then the parameter n has a most probable value of -0.5 . However, no value of n could be found for which Eq. (4) gives a good description of the data.

The significance of the results illustrated in Figs. 8 and 9 is not clear, since the median energy of the neutrons used in these experiments, approximately 2–3 MeV, is such that contributions from direct interactions are not expected to be important. However, for the neutron energies used, and for the nuclear levels studied in these experiments, it seems clear that a correlation does exist between the probability of exciting a nuclear state by neutron inelastic scattering and the reduced quadrupole transition probability, $B(E2)$, of that state.

ACKNOWLEDGMENTS

The author thanks Dr. P. Signell, who prepared the computer program used in the statistical analyses of the data, and the members of the Pennsylvania State reactor operating staff, who provided the neutrons.

Optical Model in the Interior of the Nucleus*

I. E. MCCARTHY

Department of Mathematical Physics, University of Adelaide, Adelaide, South Australia

(Received June 25, 1962)

It is shown how phase relationships between partial waves in the optical model result in focusing effects which are largest for surface partial waves. In the case of very low incident energies where the wavelength of a partial wave is large compared to the nuclear surface thickness, it is shown how the phase relationships may enable surface- and volume-reaction mechanisms for a direct reaction to be distinguished by looking at gross features of the angular distribution. Thus, low-energy direct interactions may be used as a probe for the nuclear interior.

1. INTRODUCTION

IT is well known that elastic scattering cross sections are sensitive only to the optical-model potential in the nuclear surface.¹ However, it is also true that optical-model wave functions calculated in potentials which fit elastic scattering data are not negligibly small in the nuclear interior² even for incident particles such as deuterons or α particles which may be expected on

physical grounds to lose their identity when they get into the interior. One would, of course, expect the physical breakup of the particle to contribute to the imaginary part of the potential so that the model should give a good estimate of the probability of finding a particle inside.

This apparent contradiction has led some people to consider that the optical model must be regarded more as a parametrization of elastic scattering than as a physical description of a nuclear reaction. The success of the distorted-wave Born approximation for direct interactions, which consists of a sum of overlap integrals involving the optical-model wave function in the vicinity of the nucleus, shows that the wave function

* Supported by the Australian Atomic Energy Commission and the Australian Institute for Nuclear Science and Engineering.

¹ J. S. Nodvik, *Proceedings of the International Conference on the Nuclear Optical Model, Florida State University Studies, No. 32* (The Florida State University, Tallahassee, 1959), p. 16; G. Igo, *Phys. Rev.* **115**, 1665 (1959).

² I. E. McCarthy, *Nuclear Phys.* **10**, 583 (1959).